**2018 International Explosives Safety Symposium & Exposition**
San Diego, CA
August 6-9, 2018

# Ballistic Trajectory Modeling for the Insensitive Munitions Type IV/V Hazardous Fragment Threshold

**Kevin T. Miers*, Daniel J. Pudlak, Brian E. Fuchs**

**US Army RDECOM-ARDEC, RDAR-MEE-W, Picatinny, NJ 07806**
***Kevin Miers, (973) 724-1180, kevin.t.miers.civ@mail.mil**

(U) Currently, the 20J fragment projection curve in TB-700-2 [1] (which also appears in AOP-39 [2]) is being used by the Insensitive Munitions (IM) community to distinguish between Type IV (deflagration) and Type V (burn) responses, in conjunction with other experimental evidence. Each fragment is collected after an IM test, and its distance from the origin is compared to a critical throw distance which depends on its mass, defined by the 20J curve. If this distance is exceeded for any of the fragments, the reaction is deemed a Type IV. Substantial resources are being expended to obtain Type V reactions for various munition systems, and thus it is important for this criterion to be meaningful and sufficiently accurate, while also being practical and inexpensive to use.

(U) The current 20J curve is relatively restrictive in the sense that it is too mass-dependent, and thus causes Type IV designations due to large, slow-moving fragments which do not appear to be dangerous. For this reason, various efforts have recently been undertaken by the community to come up with an improved and more meaningful criterion for what a Type V should indicate. Some matters of contention included the intent of the curve (severity and mechanism of injury), the appropriate hazard metric (energy, energy per unit area, etc.), the conditions at which the metric applies (launch, impact, impact at some distance), if and how the criterion should vary for different shapes and materials, how many fragments must fail the criterion before a Type IV is declared, and the meaning of a 15m distance requirement which appears frequently in the documents [1, 2]. These ambiguities led to some exploratory trajectory modeling being performed to try to reproduce the curve, as there was no documentation available which adequately explained its origin. A point mass ballistic trajectory code similar to TRAJ [5] and a univariate optimization tool were written and validated for this purpose. It was found that the curve in [1, 2] represents the maximum distance a chunky steel warhead fragment [4] could travel with a 20J launch energy. While a 20J impact energy curve would be desirable, the hazardous distances associated with non-negligibly small masses become unbounded.

(U) The community decided to keep 20J as the hazard metric, but changed it to a 20J impact at 15m criterion, with a different curve for each of several fragment densities. This curve guarantees that if the criterion is violated, a person standing at 15m would be hit with a 20J impact if the trajectory were lowered. The authors have constructed the mass-distance curves being incorporated into the new version of AOP-39. This paper documents the methodology and assumptions involved in generation of the new curves. It is hoped that this work will help elucidate the details and limitations of the criterion as well as areas in which potential improvements can be made, since the criterion is currently of significant consequence to the success or failure of various IM programs.

## (U) Background and Objectives

(U) All U.S. munitions are required by international agreement to be made Insensitive Munitions (IM) compliant to the extent practical. This entails that the munition in both its operational and logistical configurations must react nonviolently when subjected to a wide array of simulated threats encountered on the modern battlefield. These include fragment and bullet impact (FI/BI), fast and slow cookoff (FCO/SCO), sympathetic reaction (SR), and shaped charge jet impact (SCJI). Response severity is categorized as follows: detonation (Type I), partial detonation (Type II), explosion (Type III), deflagration (Type IV), and burn (Type V). The determination of reaction severity is made based on photographic evidence, witness plate damage, fragment size and throw distance, and blast gauge pressure readings.

(U) Currently, the 20J curve in TB-700-2 [1], which also appears in AOP-39 [2], is being used by the IM community to distinguish between Type IV (deflagration) and Type V (burn) responses. Fragments are picked up on the range after an IM test, and their distance from the origin compared to a critical throw distance, defined by the 20 curve, corresponding to the mass of each fragment. If this critical distance is exceeded, it is judged a Type IV. If this distance is not exceeded, it is judged a Type V (as long as other criterion are satisfied, such as absence of blast overpressure and witness plate gouging). The 20J curve as seen in AOP-39 and TB-700-2 is shown in Figure 1.

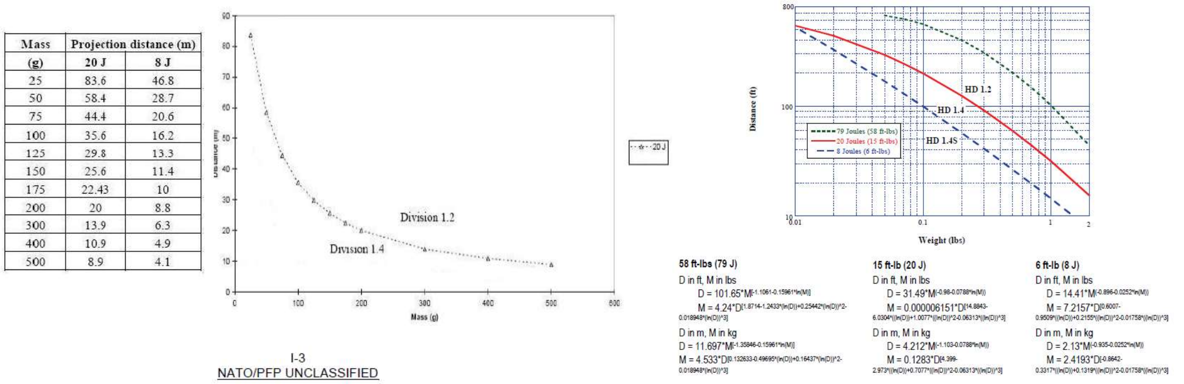

| Mass | Projection distance (m) | |
|---|---|---|
| (g) | 20 J | 8 J |
| 25 | 83.6 | 46.8 |
| 50 | 58.4 | 28.7 |
| 75 | 44.4 | 20.6 |
| 100 | 35.6 | 16.2 |
| 125 | 29.8 | 13.3 |
| 150 | 25.6 | 11.4 |
| 175 | 22.43 | 10 |
| 200 | 20 | 8.8 |
| 300 | 13.9 | 6.3 |
| 400 | 10.9 | 4.9 |
| 500 | 8.9 | 4.1 |

I-3
NATO/PFP UNCLASSIFIED

**58 ft-lbs (79 J)**
D in ft, M in lbs
$D = 101.65*M^{[-1.1061-0.15961*\ln(M)]}$
$M = 4.24*D^{[1.8714-1.2433*(\ln(D))+0.25442*(\ln(D))^2-0.018948*(\ln(D))^3]}$
D in m, M in kg
$D = 11.697*M^{[-1.35846-0.15961*\ln(M)]}$
$M = 4.533*D^{[0.132633-0.49695*(\ln(D))+0.16437*(\ln(D))^2-0.018948*(\ln(D))^3]}$

**15 ft-lb (20 J)**
D in ft, M in lbs
$D = 31.49*M^{(-0.98-0.0788*\ln(M))}$
$M = 0.000006151*D^{[14.8843-6.0304*((\ln(D))+1.0077*((\ln(D))^2-0.06313*((\ln(D))^3]}$
D in m, M in kg
$D = 4.212*M^{(-1.103-0.0788*\ln(M))}$
$M = 0.1283*D^{[4.399-2.973*((\ln(D))+0.7077*((\ln(D))^2-0.06313*((\ln(D))^3]}$

**6 ft-lb (8 J)**
D in ft, M in lbs
$D = 14.41*M^{(-0.896-0.0252*\ln(M))}$
$M = 7.2157*D^{[0.6007-0.9509*((\ln(D))+0.2155*((\ln(D))^2-0.01758*((\ln(D))^3]}$
D in m, M in kg
$D = 2.13*M^{(-0.935-0.0252*\ln(M))}$
$M = 2.4193*D^{[-0.8642-0.3317*((\ln(D))+0.1319*((\ln(D))^2-0.01758*((\ln(D))^3]}$

**(U) Figure 1 – The 20J Curve, as it appears in AOP-39 (left) and TB-700-2 (right)**

(U) Substantial resources are being expended to obtain Type V responses. However the 20J curve is currently too restrictive in the sense that it is too mass-dependent, and thus causes Type IV designations due to large, slow-moving fragments that are intuitively thought not to be dangerous. For this reason efforts were being undertaken by the community to come up with a better and more meaningful criterion for what a Type V should be. Discussions were had about whether the 20J curve should be used, or if the 79J curve in TB-700 should be used instead as a better indicator of, for example, danger to personnel. In doing so, there became confusion about what these curves meant, and there were conflicting reports indicating that the 20J referred to launch energy, impact energy, or something else. Additionally, a “20J at 15m” caveat is associated with the standard in some sources, which is also of ambiguous origin and adds additional confusion.

(U) These ambiguities led to some exploratory trajectory modeling being performed to try to reproduce the curves. A point mass ballistic trajectory code was written, validated and utilized to try various approaches to pinpoint what the curves might represent (launch energy, impact energy, or something else) and why such a criterion was chosen. There was no documentation the authors were aware of which adequately explained the origin of these curves. The outcome of this modeling was that the 20J curve seemed to represent launch energy, and the 79J curve could not be reproduced in spite of considerable effort. When this was discovered, the originators of the curves were eventually contacted to explain what was done. An explanation for the 20J curve was provided, and it was discovered to be in error compared to the outcome that was intended. An explanation for the 79J curve could not be provided.

(U) After some deliberation the community decided to keep 20J as the lethality metric but changed it to a 20J impact at 15m criterion for different fragment densities. The authors have constructed the curve being incorporated into the new version of AOP-39. This paper documents the methodology and assumptions which are built into the generation of the new curve, as well as its limitations. It is hoped that this work will help bring attention to the state of the criterion and areas in which potential improvements can be made, since the criterion is currently of significant consequence to the success or failure of various IM programs.

## (U) Aeroballistic Trajectory Modeling

(U) Air drag is the primary consideration in determining whether debris from an explosion is hazardous. The so-called point mass model can be used to determine the trajectory of a fragment launched with a given velocity and angle if some parameters about the mass, size and shape of the fragment are known [3]. It is a vector equation which assumes the drag force to act against the direction of motion (with no wind assumed), as follows:

$$\frac{d\boldsymbol{V}}{dt} = -\frac{\rho S C_D}{2m}|\boldsymbol{V}|\boldsymbol{V} + \boldsymbol{g} \tag{1a}$$

$$\frac{d\boldsymbol{x}}{dt} = \boldsymbol{V} \tag{1b}$$

Where **V** is the velocity vector, |**V**| is its magnitude, **x** is the position vector, **g** is the acceleration of gravity, ρ is the density of air, $S$ is the presented area of the projectile, $C_D$ is the drag coefficient which is in general a function of the Mach number $M$, and $m$ is the projectile mass. The system of first-order ordinary differential equations given by equation (1a) is nonlinear and autonomous, meaning the right-hand side (RHS) is a function of **V** only. Then the system represents a time-independent direction field in phase space, and each initial condition has a unique trajectory. The system has a critical point where the RHS is zero (corresponding to terminal velocity) and its Jacobian there has real negative eigenvalues and two independent eigenvectors. This indicates that the system is asymptotically stable, and all trajectories terminate at the critical point. In addition nullclines appear where $dV_x/dt = 0$ or $dV_y/dt = 0$. Direction fields for equation (1a) are shown in Figure 2. The conclusion is that a trajectory calculation can be performed either forwards or backwards in time, provided the initial condition is sufficiently far from the critical points and nullclines. In the calculations to follow, this does not appear to be an issue, but backward trajectories in question should be checked for accuracy by running them forward in time.

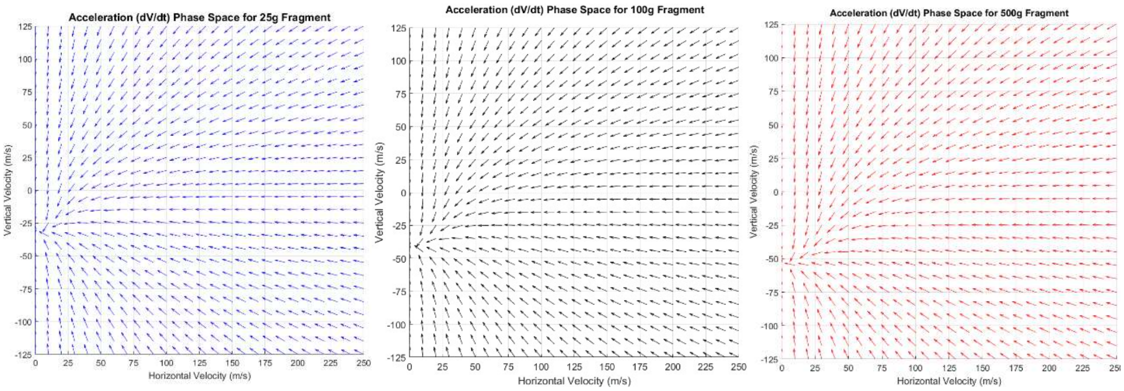

**(U) Figure 2 – Direction fields for Eq. (1a) with 25g, 100g, and 500g steel fragments**

(U) Wind effects might also be present, as well as ricochets off the ground. These effects can be included in the analysis if desired, but this work does not include them. In general these equations are coupled and nonlinear, and have no analytical solution. Analytical solutions do exist for small launch angles with certain functional variations of the drag coefficient with Mach number (the so-called "flat fire" assumption) and vertical launch. Thus the analytical solutions can be used as a check to verify that the numerical solution of these equations is implemented correctly.

(U) Trajectory calculations require the density of air, drag coefficient, mass, and presented area of the fragment to be known. The density of air varies slightly with temperature and pressure, so a standard density of 1.2 kg/m$^3$ is used. Fragments from an explosion are irregularly shaped and tumble through the air, and thus the presented areas and drag coefficients can vary wildly. Additionally, the drag coefficient of a given shape varies with Mach number. To try to take these complications into account, there are two approximations that are generally used for fragment trajectories: a functional dependence of drag coefficient on Mach number, and a functional dependence of presented area on mass. The drag coefficient vs. Mach number data for chunky fragments, which was taken from [4] to generate the curves, is shown in Figure 3. It also turns out to be the default drag data used in the TRAJ program [5]. It should be noted that for hypersonic velocities (M>5) a constant drag coefficient is considered a reasonable assumption [3], although the exact Mach number at which this data becomes invalid is unknown. Therefore in general the Mach number should be monitored when doing a fragment projection analysis to ensure valid results, although for the 20J curves this is never a concern.

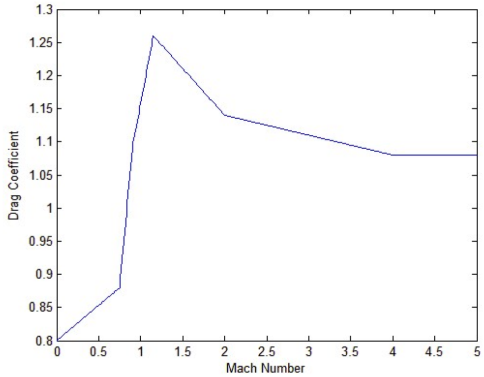

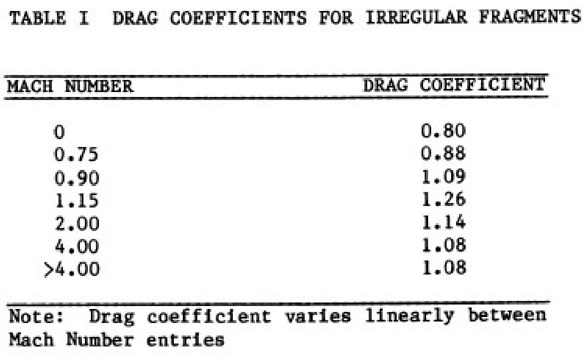
TABLE I DRAG COEFFICIENTS FOR IRREGULAR FRAGMENTS

| MACH NUMBER | DRAG COEFFICIENT |
|---|---|
| 0 | 0.80 |
| 0.75 | 0.88 |
| 0.90 | 1.09 |
| 1.15 | 1.26 |
| 2.00 | 1.14 |
| 4.00 | 1.08 |
| >4.00 | 1.08 |

Note: Drag coefficient varies linearly between Mach Number entries

**(U) Figure 3 – Drag coefficient variation with Mach number used in the analysis [4]**

(U) If the shape and orientation of a projectile is known, $S$ in Equation 1a is simply its presented area. However in computing ballistic trajectories for irregularly shaped, randomly tumbling fragments, $S$ is typically taken to be the average presented area. For an arbitrary convex shape, the average presented area is well-known to be ¼ of its total surface area and can be calculated as such. However for fragments from naturally fragmenting warheads the average presented area is typically assumed to depend on the fragment mass functional form which is as follows:

$$m = kS^{3/2} \tag{2}$$

To determine $k$ experimentally for a given weapon, the average presented area has historically been measured using an icosahedron gage. Values of 2600 kg/m$^3$ for fragmentation bombs and 2300 kg/m$^3$ for demolition bombs are found in [6].

(U) The shape factor for steel warhead fragments is likely to perform poorly in the prediction of trajectories for fragments of shapes, sizes and densities different from steel warhead fragments. The drag coefficient data is also expected to differ for such debris. Fortunately, $k$ can at least be modified to take into account the density of the fragment. For a fragment of a fixed size and shape, the shape factor is proportional to the fragment density, shown in equation (3).

$$m = kS^{3/2} \Rightarrow \rho V_{frag} = kS_{frag}^{3/2} \Rightarrow k = \frac{V_{frag}}{S_{frag}^{3/2}}\rho \equiv K\rho \tag{3}$$

(U) Limited correspondence with the originators of the curves indicated that a “chunky fragment with a shape factor of 0.33” was used. This likely refers to “B” in the following from [4, 5]:

$$m = \rho BAL \tag{4}$$

In equation (4) the shape factor $B$ refers to the ratio of the actual fragment volume to the volume of the smallest rectangular box that can enclose the fragment. Then $A$ is the presented area of the box, $L$ is the box length in the direction of travel, and $\rho$ is the density of the fragment. This is the formulation used in the TRAJ code. In general $AL$ is not equal to $S^{3/2}$, but assuming it is results in

$$k = \rho B \tag{5}$$

which evaluates to ~2600 kg/m$^3$ for steel fragments with $B$=0.33. Use of $k$=2600 kg/m$^3$ gives excellent agreement with codes such as TRAJCAN. If a particular orientation of a projectile is assumed, and its mass and presented area are known, it is unnecessary to go through the shape factor model. In any case, the value of $k$ being used in the legacy criterion is for steel fragments which resulted from a detonating warhead. Fragments resulting from sub-detonative responses commonly observed in IM tests can easily violate this assumption.

(U) The trajectories were solved numerically using MATLAB’s “ode45” function [7]. The error tolerances (*AbsTol* and *RelTol*) were reduced to 1e-9 from their default values of 1e-3 to ensure accurate solutions. An event handler stops the integration at the timestep where the trajectory ordinate becomes negative, and the impact point is determined by linearly interpolating the trajectory between this timestep and the one immediately before it. The drag data was implemented as a linear interpolation between various points on the $C_D$ vs. M curve, which evaluates the drag coefficient based on the Mach number at each timestep. Details of the implementation and testing of this code can be found in [8], and it appears to accurately reproduce flat-fire analytical solutions as well as the outputs of several other computer programs.

## (U) Lethality Criteria

(U) The objective of IM is to design munitions with exceptional lethality performance which do not react violently when subjected to ballistic and thermal threats commonly encountered in modern warfare. This is a difficult endeavor as higher-performance energetic materials are often more susceptible to violent reaction due to unplanned stimuli. IM is concerned with improving warfighter survivability in a combat scenario, although it provides important safety benefits as well. As such the survivability improvement gained from safer weapons must outweigh the opportunity cost of potentially more effective logistics operations and better performance. In this unique situation, improving munition system safety to the point that it too negatively affects combat effectiveness results in an overall decrease in survivability. Conversely, if munitions subjected to impacts and fires are allowed to react violently enough to have a high probability of causing damage and casualties which generate additional logistical burdens and IM hazards, survivability is doubly affected. As a result there ought to be an optimal level of acceptable hazard appropriate for IM design requirements, which is partially borne out in the fragment projection hazard criterion. It is a personnel hazard criterion, which might not be the only hazard worth considering but is in any case a conservative one. Clearly personnel hazard at an arbitrary distance is a poor metric of reaction violence, but attempting to reduce personnel hazard is why energetic reaction types are assigned in the first place [11]. Injury severity is often measured as an Abbreviated Injury Scale (AIS) score, and an appropriate one should be agreed upon by the IM community. Based on various discussions, a requirement similar to AIS 2 (moderate injury with 1-2% probability of death) is often favored, however a strong rationale for using this score is not usually provided.

(U) Currently the hazard criterion being used in the analysis is 20J. However, since there is much debate over whether this criterion is adequate, an energy density criterion was also considered. Utilizing an energy per unit area (energy density) criterion would seem an intuitive way to separate hazardous and nonhazardous impacts. What would be considered hazardous ought to vary wildly with the mass, material, geometry and hit location of the projectile. Impacts of sharp projectiles to fragile body areas would appear quite hazardous at low velocities. However besides introducing new and potentially burdensome data collection requirements for each fragment, [9] suggests that such a criterion is not conservative for masses above approximately 100g because the mechanism of injury becomes blunt trauma. They suggest, based on their own lethality modeling, that energy alone is a better indicator of this mechanism, and that 20J is a comfortably conservative number to use to prevent serious injury due to blunt trauma. Except for several old papers which suggested a skin penetration energy density of 7.9 $J/cm^2$, we were not able to locate any data in the open literature to confirm or dispute this. In any case, the 7.9 $J/cm^2$ criteria resulted in throw distances so large as to render the mass-distance curve mostly useless, as is discussed a subsequent section. Lethality modeling is currently being performed for the fragment masses of interest using state-of-the-art US simulation tools which take various types of injury and higher fidelity aeroballistics information into account.

## (U) Line Search Algorithms

(U) The numerical solution of the equations of motion provides a numerical output (landing conditions) as a function of a numerical input (launch conditions). In calculating the curves we often have to calculate maximum or minimum output quantities. Some of these include maximum distance for a given launch velocity, maximum distance for a given impact velocity, or minimum launch velocity to hit 15m with 20J. This can be done manually by, for instance, adjusting the launch angle until the maximum distance is found. However this is tedious and potentially inaccurate. Additionally, if for instance a particular impact velocity and throw distance are simultaneously desired, the launch angle and launch velocity would both need to be varied to achieve this. Fortunately, the ability to run trajectories backward in time from impact eliminates this difficulty. Efficiently searching for maxima or minima of an objective function using only numerical inputs and outputs is sometimes referred to as "nonlinear optimization". Algorithms to locate extreme values in a single dimension are referred to as "line searches".

(U) In particular there exist several highly efficient and well-established line search algorithms for so-called "unimodal" objective functions, which have a single maximum/minimum that all other points monotonically increase/decrease toward [10]. Some of these algorithms include simple bisection, the Fibonacci search, and the golden section search. If the objective function is known to be unimodal over a given interval, these algorithms may be applied directly. However if the objective function is not known to be unimodal, a local extremum near the starting point can be located by progressively extending the prospective search interval until the value of the objective function begins to increase, at which point the extremum has been bracketed and the objective function is unimodal over that interval. A line search is then performed within that interval to exactly determine the extreme value. In this work a simple bisection method is utilized for performing line searches, since evaluation of the ballistic trajectories is not very computationally intensive. Additionally it is robust and simple to program. Most of the objective functions of interest in this work are unimodal.

## (U) Mass-Distance Curves and the AOP-39 Fragment Projection Criterion

(U) The new fragment projection criterion is 20J impact at 15m for several different fragment densities. It is a throw distance (ordinate) vs. mass (abscissa) curve which indicates that if the specified distance is exceeded for a fragment of a given mass (i.e., the criterion is violated), the fragment is guaranteed to have been launched with at least the minimum velocity required to impact 15m with 20J. It does not guarantee the actual impact was hazardous, but does guarantee that it would have been hazardous at 15m if the trajectory was lowered. A graphical representation of this is shown in Figure 4. The throw distance calculation is repeated for each fragment mass and density of interest, and is performed in two steps. First, the minimum launch velocity to hit the ground at 15m with a 20J impact is found. Then using that launch velocity, the launch angle is adjusted until the maximum distance is found. This is the distance which is used in the criterion, presented later in the paper. Also, if a mass is so large that it impacts with >20J at the minimum launch velocity to reach 15m, the curve is cut off at 15m. This is not an arbitrary cutoff because a person standing at 15m is still guaranteed to be hit with >20J if such a fragment is found at 15m; closer distances are considered irrelevant. This criterion first appeared in [9].

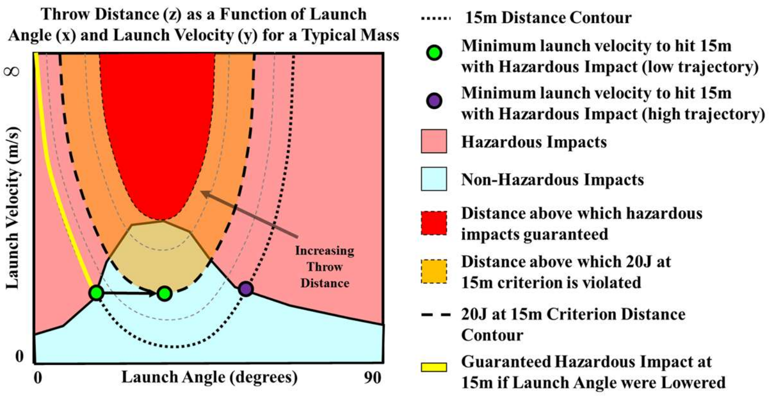

**(U) Figure 4 – Graphical representation implications of 20J impact at 15m curve. Throw distance (z) plotted as a function of launch angle (x) and launch velocity (y) for a typical fixed mass. Color coded by whether impact was hazardous (pink) or not (blue).**

(U) This is different from a 20J impact or 20J launch curve, which represents the largest distance a fragment of a given mass could travel having been launched or having impacted with 20J. The distances for the 20J impact at 15m curve end up being slightly larger than for the 20J launch curve. A 20J impact curve independent from the 15m restriction would be desirable since it guarantees hazardous impacts if violated. However below non-negligibly small masses (~50g for 20J impacts, ~125g for 79J impacts) the distances become very large and go off to infinity, shown in Figure 5. This is because smaller projectiles drag down significantly faster than large projectiles, and below a certain mass are never hazardous on impact at maximum range.

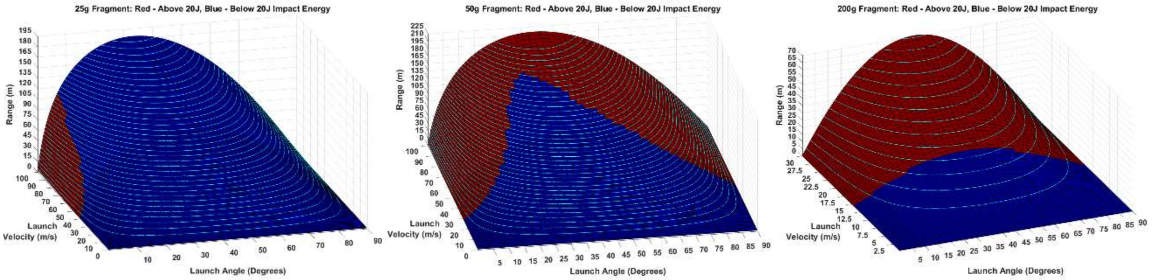

**(U) Figure 5 – State space searches for 20J hazard criterion (red indicates hazardous impacts, blue indicates non-hazardous impacts)**

(U) The most important problem with the mass-distance curves is that the curve becomes less meaningful the higher the allowable throw distances become. Mass-distance curves represent the maximum range a fragment with a given hazard criterion could possibly travel. Thus fragments that lie above the curve are guaranteed to be hazardous. However, the fragments that lie below the curve are *not* guaranteed *not* to be hazardous. This can be easily verified by launching a highly energetic fragment either vertically or directly at the ground. Thus as the hazard criterion is made less conservative, the ability to detect hazardous fragments is reduced. This consideration is as important as, if not more important than, the hazard criterion itself. If the distances specified by the curve are too large, and all the fragments lie below the curve, no useful information has been obtained. Indeed, for impact curves not associated with a distance (e.g., 15m), nothing can be concluded at all about fragments below a given mass. In addition errors in the modeling assumptions have more of an influence on the answers as the throw distances are increased.

(U) Finally, for the probability of being hit while standing 15m away to be 1%, ~25 fragments would have to be thrown in random directions, assuming straight trajectories which are equally likely. Thus it would seem to make sense to allow a certain number of fragments to fail the criterion before declaring a hazardous energetic reaction. However, logistical configurations containing many munition items may project more debris for the same reaction, as appears noted in [9].

(U) We are thus driven toward a more conservative criterion. The best we can do with the mass-distance curves is to ensure a low probability that a bystander is definitely exposed to hazardous fragments, rather than guaranteeing that a bystander is safe [11]. While the community has decided to stay with 20J as a hazard criterion for now, it is worth examining whether a somewhat different hazard criterion might be more appropriate, as well as how seriously violations of the criterion should be taken. This could potentially provide much-needed relief to IM programs without the standard becoming much less meaningful.

## (U) Calculation of the Curves

(U) The first step in calculating the curve is to search for the minimum launch velocity which could hit a person standing at 15m with a 20J fragment. The easiest way to do this is to search backward in time from the 20J impact at 15m, adjusting the impact angle until the trajectory intersects the origin. If the fragment was launched from a test stand (assumed to be 1m high), there are two ways to handle relocating the origin to the top of the test stand. A simple approximation that is easy to code is to assume the fragment impacts the person standing at 15m at the same height as the test stand. However in this case the cutoff for large masses is not 15m, but rather 15m plus the distance a fragment travels as it falls the extra 1m. This manifests itself as a small discontinuity in the curve near the cutoff. An easy way to handle the test stand is to assume the impact plane is a vertical wall at the origin and do a line search in the impact height for 1m off the ground. This simplified programming the event handler in the code since it is triggered only once for any trajectory. This was somewhat more involved to program but yielded the required answers.

(U) A description of the code used to perform the first step is as follows. The impact angle is assumed to start at zero, and is increased until the 1m launch height is exceeded. The absolute value of the distance between the current launch height and 1m is then minimized using a line search. It should also be noted that in general there are two trajectories which impact 15m at 20J, and thus the objective function is not strictly unimodal. The low trajectory usually produces a lower launch velocity to hit 15m, except for the larger masses. For some lower masses there is no high trajectory solution. Both trajectories are calculated, and the lowest launch velocity trajectory is used in the curve output. It should be noted that the error in the curve output is at most ~1m if the low trajectory is used exclusively. If the maximum launch height in the plane of the origin is below 1m, there is no trajectory connecting the test stand and the ground at 15m which can result in an impact of 20J. A cutoff of 15m is used for the curve in this case. The output of this first step is the launch velocity from the test stand required to hit the ground at 15m with exactly 20J. A diagram of the line search is shown in Figure 6.

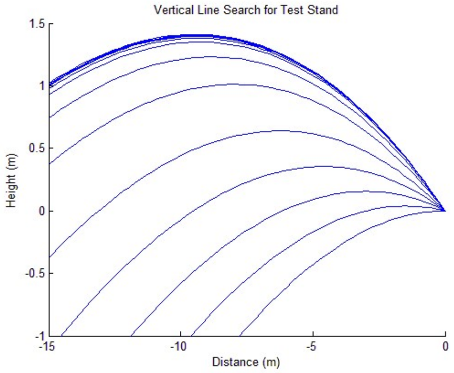

**(U) Figure 6 – Vertical line search for test stand**

(U) The second step holds fixed the launch velocity determined in the first step, and varies the launch angle to determine the maximum distance a fragment could travel (forward in time from atop the test stand) if launched at that velocity. This resulting maximum distance is then recorded as a point on the final mass-distance curve. This entire procedure is repeated for each fragment mass, yielding the new 20J impact at 15m curves which are shown in Figure 7.

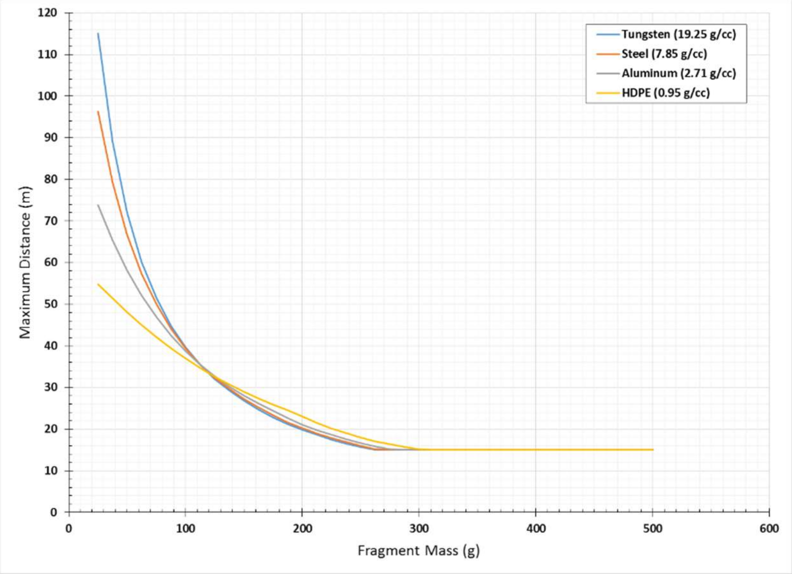

**(U) Figure 7 – New AOP-39 mass-distance curve**

(U) The crossover in the curves for the different densities is somewhat non-intuitive but makes sense. For small masses, the launch velocity required to impact 15m at 20J is large and the trajectories are relatively flat, so raising the angle for the second step results in a substantial increase in distance in which case denser fragments travel further. For larger masses, the velocities involved are lower, drag has less of an effect, and the trajectories are comparable in both steps. However less dense materials require a larger launch velocity to reach 15m with 20J in the first step. This higher launch velocity "wins out" for less dense materials when the launch angle is raised for the second step. The slight "knee" in the curves, most noticeable for HDPE, appears where the high trajectory begins to produce the lower minimum launch velocity. The cutoff at 15m is applied when the masses are so large that they impact with at least 20J by virtue of traveling

15m. The output values are listed in Figures 8-11. The launch energy is slightly less than the impact energy for some of the larger masses because of the 1m test stand.

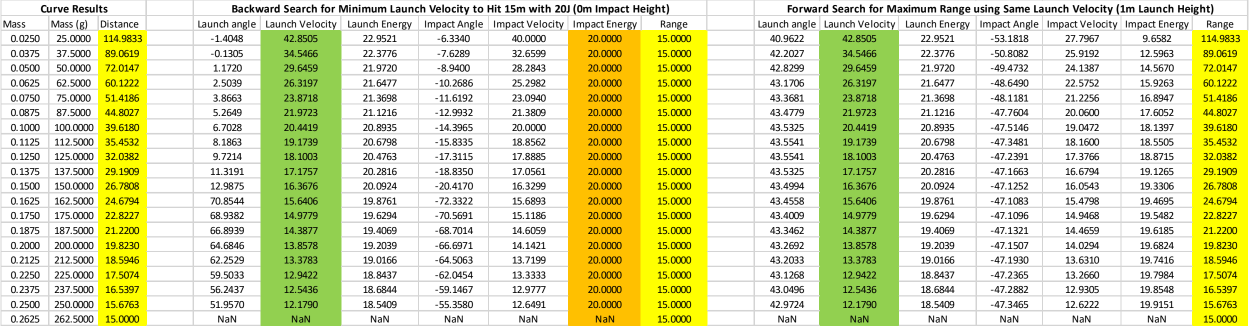

| Curve Results | | | Backward Search for Minimum Launch Velocity to Hit 15m with 20J (0m Impact Height) | | | | | | | Forward Search for Maximum Range using Same Launch Velocity (1m Launch Height) | | | | | | |
|---|---|---|---|---|---|---|---|---|---|---|---|---|---|---|---|---|
| Mass | Mass (g) | Distance | Launch angle | Launch Velocity | Launch Energy | Impact Angle | Impact Velocity | Impact Energy | Range | Launch angle | Launch Velocity | Launch Energy | Impact Angle | Impact Velocity | Impact Energy | Range |
| 0.0250 | 25.0000 | 114.9833 | -1.4048 | 42.8505 | 22.9521 | -6.3340 | 40.0000 | 20.0000 | 15.0000 | 40.9622 | 42.8505 | 22.9521 | -53.1818 | 27.7967 | 9.6582 | 114.9833 |
| 0.0375 | 37.5000 | 89.0619 | -0.1305 | 34.5466 | 22.3776 | -7.6289 | 32.6599 | 20.0000 | 15.0000 | 42.2027 | 34.5466 | 22.3776 | -50.8082 | 25.9192 | 12.5963 | 89.0619 |
| 0.0500 | 50.0000 | 72.0147 | 1.1720 | 29.6459 | 21.9720 | -8.9400 | 28.2843 | 20.0000 | 15.0000 | 42.8299 | 29.6459 | 21.9720 | -49.4732 | 24.1387 | 14.5670 | 72.0147 |
| 0.0625 | 62.5000 | 60.1222 | 2.5039 | 26.3197 | 21.6477 | -10.2686 | 25.2982 | 20.0000 | 15.0000 | 43.1706 | 26.3197 | 21.6477 | -48.6490 | 22.5752 | 15.9263 | 60.1222 |
| 0.0750 | 75.0000 | 51.4186 | 3.8663 | 23.8718 | 21.3698 | -11.6192 | 23.0940 | 20.0000 | 15.0000 | 43.3681 | 23.8718 | 21.3698 | -48.1181 | 21.2256 | 16.8947 | 51.4186 |
| 0.0875 | 87.5000 | 44.8027 | 5.2649 | 21.9723 | 21.1216 | -12.9932 | 21.3809 | 20.0000 | 15.0000 | 43.4779 | 21.9723 | 21.1216 | -47.7604 | 20.0600 | 17.6052 | 44.8027 |
| 0.1000 | 100.0000 | 39.6180 | 6.7028 | 20.4419 | 20.8935 | -14.3965 | 20.0000 | 20.0000 | 15.0000 | 43.5325 | 20.4419 | 20.8935 | -47.5146 | 19.0472 | 18.1397 | 39.6180 |
| 0.1125 | 112.5000 | 35.4532 | 8.1863 | 19.1739 | 20.6798 | -15.8335 | 18.8562 | 20.0000 | 15.0000 | 43.5541 | 19.1739 | 20.6798 | -47.3481 | 18.1600 | 18.5505 | 35.4532 |
| 0.1250 | 125.0000 | 32.0382 | 9.7214 | 18.1003 | 20.4763 | -17.3115 | 17.8885 | 20.0000 | 15.0000 | 43.5541 | 18.1003 | 20.4763 | -47.2391 | 17.3766 | 18.8715 | 32.0382 |
| 0.1375 | 137.5000 | 29.1909 | 11.3191 | 17.1757 | 20.2816 | -18.8350 | 17.0561 | 20.0000 | 15.0000 | 43.5325 | 17.1757 | 20.2816 | -47.1663 | 16.6794 | 19.1265 | 29.1909 |
| 0.1500 | 150.0000 | 26.7808 | 12.9875 | 16.3676 | 20.0924 | -20.4170 | 16.3299 | 20.0000 | 15.0000 | 43.4994 | 16.3676 | 20.0924 | -47.1252 | 16.0543 | 19.3306 | 26.7808 |
| 0.1625 | 162.5000 | 24.6794 | 70.8544 | 15.6406 | 19.8761 | -72.3322 | 15.6893 | 20.0000 | 15.0000 | 43.4558 | 15.6406 | 19.8761 | -47.1083 | 15.4798 | 19.4695 | 24.6794 |
| 0.1750 | 175.0000 | 22.8227 | 68.9382 | 14.9779 | 19.6294 | -70.5691 | 15.1186 | 20.0000 | 15.0000 | 43.4009 | 14.9779 | 19.6294 | -47.1096 | 14.9468 | 19.5482 | 22.8227 |
| 0.1875 | 187.5000 | 21.2200 | 66.8939 | 14.3877 | 19.4069 | -68.7014 | 14.6059 | 20.0000 | 15.0000 | 43.3462 | 14.3877 | 19.4069 | -47.1321 | 14.4659 | 19.6185 | 21.2200 |
| 0.2000 | 200.0000 | 19.8230 | 64.6846 | 13.8578 | 19.2039 | -66.6971 | 14.1421 | 20.0000 | 15.0000 | 43.2692 | 13.8578 | 19.2039 | -47.1507 | 14.0294 | 19.6824 | 19.8230 |
| 0.2125 | 212.5000 | 18.5946 | 62.2529 | 13.3783 | 19.0166 | -64.5063 | 13.7199 | 20.0000 | 15.0000 | 43.2033 | 13.3783 | 19.0166 | -47.1930 | 13.6310 | 19.7416 | 18.5946 |
| 0.2250 | 225.0000 | 17.5074 | 59.5033 | 12.9422 | 18.8437 | -62.0454 | 13.3333 | 20.0000 | 15.0000 | 43.1268 | 12.9422 | 18.8437 | -47.2365 | 13.2660 | 19.7984 | 17.5074 |
| 0.2375 | 237.5000 | 16.5397 | 56.2437 | 12.5436 | 18.6844 | -59.1467 | 12.9777 | 20.0000 | 15.0000 | 43.0496 | 12.5436 | 18.6844 | -47.2882 | 12.9305 | 19.8548 | 16.5397 |
| 0.2500 | 250.0000 | 15.6763 | 51.9570 | 12.1790 | 18.5409 | -55.3580 | 12.6491 | 20.0000 | 15.0000 | 42.9724 | 12.1790 | 18.5409 | -47.3465 | 12.6222 | 19.9151 | 15.6763 |
| 0.2625 | 262.5000 | 15.0000 | NaN | NaN | NaN | NaN | NaN | NaN | 15.0000 | NaN | NaN | NaN | NaN | NaN | NaN | 15.0000 |

(U) Figure 8 – Output data for tungsten (19.25 g/cc)

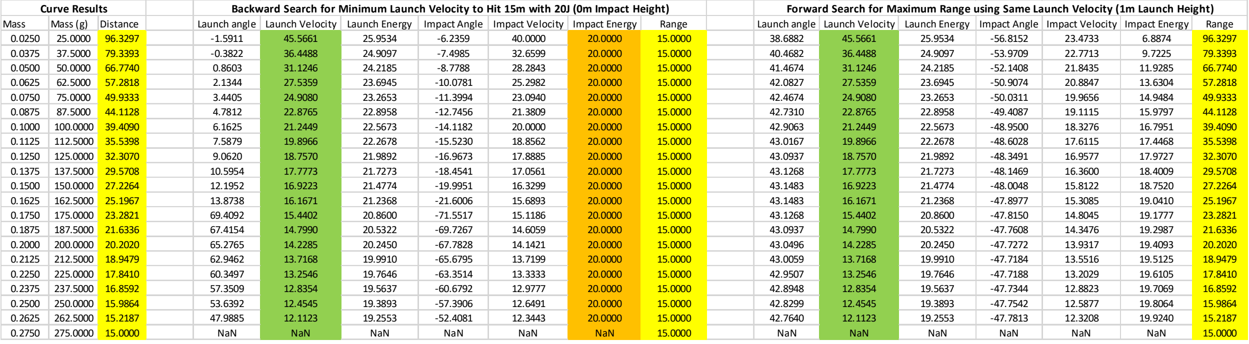

| Curve Results | | | Backward Search for Minimum Launch Velocity to Hit 15m with 20J (0m Impact Height) | | | | | | | Forward Search for Maximum Range using Same Launch Velocity (1m Launch Height) | | | | | | |
|---|---|---|---|---|---|---|---|---|---|---|---|---|---|---|---|---|
| Mass | Mass (g) | Distance | Launch angle | Launch Velocity | Launch Energy | Impact Angle | Impact Velocity | Impact Energy | Range | Launch angle | Launch Velocity | Launch Energy | Impact Angle | Impact Velocity | Impact Energy | Range |
| 0.0250 | 25.0000 | 96.3297 | -1.5911 | 45.5661 | 25.9534 | -6.2359 | 40.0000 | 20.0000 | 15.0000 | 38.6882 | 45.5661 | 25.9534 | -56.8152 | 23.4733 | 6.8874 | 96.3297 |
| 0.0375 | 37.5000 | 79.3393 | -0.3822 | 36.4488 | 24.9097 | -7.4985 | 32.6599 | 20.0000 | 15.0000 | 40.4682 | 36.4488 | 24.9097 | -53.9709 | 22.7713 | 9.7225 | 79.3393 |
| 0.0500 | 50.0000 | 66.7740 | 0.8603 | 31.1246 | 24.2185 | -8.7788 | 28.2843 | 20.0000 | 15.0000 | 41.4674 | 31.1246 | 24.2185 | -52.1408 | 21.8435 | 11.9285 | 66.7740 |
| 0.0625 | 62.5000 | 57.2818 | 2.1344 | 27.5359 | 23.6945 | -10.0781 | 25.2982 | 20.0000 | 15.0000 | 42.0827 | 27.5359 | 23.6945 | -50.9074 | 20.8847 | 13.6304 | 57.2818 |
| 0.0750 | 75.0000 | 49.9333 | 3.4405 | 24.9080 | 23.2653 | -11.3994 | 23.0940 | 20.0000 | 15.0000 | 42.4674 | 24.9080 | 23.2653 | -50.0311 | 19.9656 | 14.9484 | 49.9333 |
| 0.0875 | 87.5000 | 44.1128 | 4.7812 | 22.8765 | 22.8958 | -12.7456 | 21.3809 | 20.0000 | 15.0000 | 42.7310 | 22.8765 | 22.8958 | -49.4087 | 19.1115 | 15.9797 | 44.1128 |
| 0.1000 | 100.0000 | 39.4090 | 6.1625 | 21.2449 | 22.5673 | -14.1182 | 20.0000 | 20.0000 | 15.0000 | 42.9063 | 21.2449 | 22.5673 | -48.9500 | 18.3276 | 16.7951 | 39.4090 |
| 0.1125 | 112.5000 | 35.5398 | 7.5879 | 19.8966 | 22.2678 | -15.5230 | 18.8562 | 20.0000 | 15.0000 | 43.0167 | 19.8966 | 22.2678 | -48.6028 | 17.6115 | 17.4468 | 35.5398 |
| 0.1250 | 125.0000 | 32.3070 | 9.0620 | 18.7570 | 21.9892 | -16.9673 | 17.8885 | 20.0000 | 15.0000 | 43.0937 | 18.7570 | 21.9892 | -48.3491 | 16.9577 | 17.9727 | 32.3070 |
| 0.1375 | 137.5000 | 29.5708 | 10.5954 | 17.7773 | 21.7273 | -18.4541 | 17.0561 | 20.0000 | 15.0000 | 43.1268 | 17.7773 | 21.7273 | -48.1469 | 16.3600 | 18.4009 | 29.5708 |
| 0.1500 | 150.0000 | 27.2264 | 12.1952 | 16.9223 | 21.4774 | -19.9951 | 16.3299 | 20.0000 | 15.0000 | 43.1483 | 16.9223 | 21.4774 | -48.0048 | 15.8122 | 18.7520 | 27.2264 |
| 0.1625 | 162.5000 | 25.1967 | 13.8738 | 16.1671 | 21.2368 | -21.6006 | 15.6893 | 20.0000 | 15.0000 | 43.1483 | 16.1671 | 21.2368 | -47.8977 | 15.3085 | 19.0410 | 25.1967 |
| 0.1750 | 175.0000 | 23.2821 | 69.4092 | 15.4402 | 20.8600 | -71.5517 | 15.1186 | 20.0000 | 15.0000 | 43.1268 | 15.4402 | 20.8600 | -47.8150 | 14.8045 | 19.1777 | 23.2821 |
| 0.1875 | 187.5000 | 21.6336 | 67.4154 | 14.7990 | 20.5322 | -69.7267 | 14.6059 | 20.0000 | 15.0000 | 43.0937 | 14.7990 | 20.5322 | -47.7608 | 14.3476 | 19.2987 | 21.6336 |
| 0.2000 | 200.0000 | 20.2020 | 65.2765 | 14.2285 | 20.2450 | -67.7828 | 14.1421 | 20.0000 | 15.0000 | 43.0496 | 14.2285 | 20.2450 | -47.7272 | 13.9317 | 19.4093 | 20.2020 |
| 0.2125 | 212.5000 | 18.9479 | 62.9462 | 13.7168 | 19.9910 | -65.6795 | 13.7199 | 20.0000 | 15.0000 | 43.0059 | 13.7168 | 19.9910 | -47.7184 | 13.5516 | 19.5125 | 18.9479 |
| 0.2250 | 225.0000 | 17.8410 | 60.3497 | 13.2546 | 19.7646 | -63.3514 | 13.3333 | 20.0000 | 15.0000 | 42.9507 | 13.2546 | 19.7646 | -47.7188 | 13.2029 | 19.6105 | 17.8410 |
| 0.2375 | 237.5000 | 16.8592 | 57.3509 | 12.8354 | 19.5637 | -60.6792 | 12.9777 | 20.0000 | 15.0000 | 42.8948 | 12.8354 | 19.5637 | -47.7344 | 12.8823 | 19.7069 | 16.8592 |
| 0.2500 | 250.0000 | 15.9864 | 53.6392 | 12.4545 | 19.3893 | -57.3906 | 12.6491 | 20.0000 | 15.0000 | 42.8299 | 12.4545 | 19.3893 | -47.7542 | 12.5877 | 19.8064 | 15.9864 |
| 0.2625 | 262.5000 | 15.2187 | 47.9885 | 12.1123 | 19.2553 | -52.4081 | 12.3443 | 20.0000 | 15.0000 | 42.7640 | 12.1123 | 19.2553 | -47.7813 | 12.3208 | 19.9240 | 15.2187 |
| 0.2750 | 275.0000 | 15.0000 | NaN | NaN | NaN | NaN | NaN | NaN | 15.0000 | NaN | NaN | NaN | NaN | NaN | NaN | 15.0000 |

(U) Figure 9 – Output data for steel (7.85 g/cc)

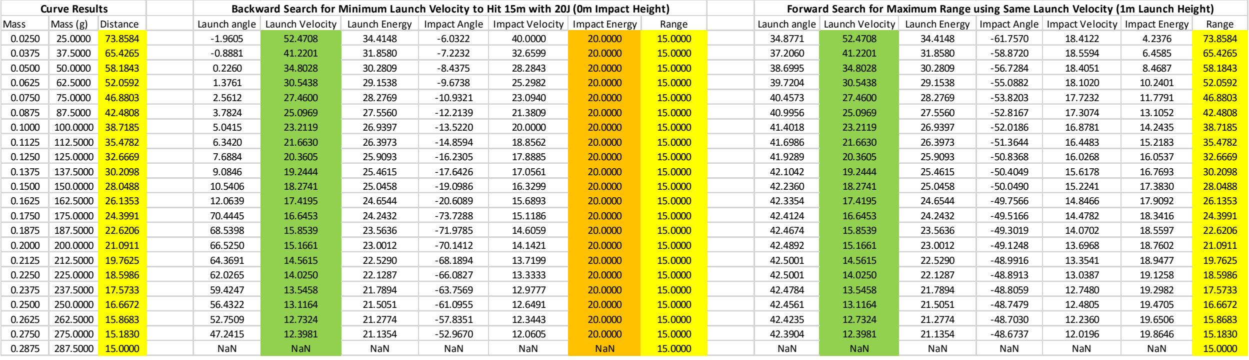

| Curve Results | | | Backward Search for Minimum Launch Velocity to Hit 15m with 20J (0m Impact Height) | | | | | | | Forward Search for Maximum Range using Same Launch Velocity (1m Launch Height) | | | | | | |
|---|---|---|---|---|---|---|---|---|---|---|---|---|---|---|---|---|
| Mass | Mass (g) | Distance | Launch angle | Launch Velocity | Launch Energy | Impact Angle | Impact Velocity | Impact Energy | Range | Launch angle | Launch Velocity | Launch Energy | Impact Angle | Impact Velocity | Impact Energy | Range |
| 0.0250 | 25.0000 | 73.8584 | -1.9605 | 52.4708 | 34.4148 | -6.0322 | 40.0000 | 20.0000 | 15.0000 | 34.8771 | 52.4708 | 34.4148 | -61.7570 | 18.4122 | 4.2376 | 73.8584 |
| 0.0375 | 37.5000 | 65.4265 | -0.8881 | 41.2201 | 31.8580 | -7.2232 | 32.6599 | 20.0000 | 15.0000 | 37.2060 | 41.2201 | 31.8580 | -58.8720 | 18.5594 | 6.4585 | 65.4265 |
| 0.0500 | 50.0000 | 58.1843 | 0.2260 | 34.8028 | 30.2809 | -8.4375 | 28.2843 | 20.0000 | 15.0000 | 38.6995 | 34.8028 | 30.2809 | -56.7284 | 18.4051 | 8.4687 | 58.1843 |
| 0.0625 | 62.5000 | 52.0592 | 1.3761 | 30.5438 | 29.1538 | -9.6738 | 25.2982 | 20.0000 | 15.0000 | 39.7204 | 30.5438 | 29.1538 | -55.0882 | 18.1020 | 10.2401 | 52.0592 |
| 0.0750 | 75.0000 | 46.8803 | 2.5612 | 27.4600 | 28.2769 | -10.9321 | 23.0940 | 20.0000 | 15.0000 | 40.4573 | 27.4600 | 28.2769 | -53.8203 | 17.7232 | 11.7791 | 46.8803 |
| 0.0875 | 87.5000 | 42.4808 | 3.7824 | 25.0969 | 27.5560 | -12.2139 | 21.3809 | 20.0000 | 15.0000 | 40.9956 | 25.0969 | 27.5560 | -52.8167 | 17.3074 | 13.1052 | 42.4808 |
| 0.1000 | 100.0000 | 38.7185 | 5.0415 | 23.2119 | 26.9397 | -13.5220 | 20.0000 | 20.0000 | 15.0000 | 41.4018 | 23.2119 | 26.9397 | -52.0186 | 16.8781 | 14.2435 | 38.7185 |
| 0.1125 | 112.5000 | 35.4782 | 6.3420 | 21.6630 | 26.3973 | -14.8594 | 18.8562 | 20.0000 | 15.0000 | 41.6986 | 21.6630 | 26.3973 | -51.3644 | 16.4483 | 15.2183 | 35.4782 |
| 0.1250 | 125.0000 | 32.6669 | 7.6884 | 20.3605 | 25.9093 | -16.2305 | 17.8885 | 20.0000 | 15.0000 | 41.9289 | 20.3605 | 25.9093 | -50.8368 | 16.0268 | 16.0537 | 32.6669 |
| 0.1375 | 137.5000 | 30.2098 | 9.0846 | 19.2444 | 25.4615 | -17.6426 | 17.0561 | 20.0000 | 15.0000 | 42.1042 | 19.2444 | 25.4615 | -50.4049 | 15.6178 | 16.7693 | 30.2098 |
| 0.1500 | 150.0000 | 28.0488 | 10.5406 | 18.2741 | 25.0458 | -19.0986 | 16.3299 | 20.0000 | 15.0000 | 42.2360 | 18.2741 | 25.0458 | -50.0490 | 15.2241 | 17.3830 | 28.0488 |
| 0.1625 | 162.5000 | 26.1353 | 12.0639 | 17.4195 | 24.6544 | -20.6089 | 15.6893 | 20.0000 | 15.0000 | 42.3354 | 17.4195 | 24.6544 | -49.7566 | 14.8466 | 17.9092 | 26.1353 |
| 0.1750 | 175.0000 | 24.3991 | 70.4445 | 16.6453 | 24.2432 | -73.7288 | 15.1186 | 20.0000 | 15.0000 | 42.4124 | 16.6453 | 24.2432 | -49.5166 | 14.4782 | 18.3416 | 24.3991 |
| 0.1875 | 187.5000 | 22.6206 | 68.5398 | 15.8539 | 23.5636 | -71.9785 | 14.6059 | 20.0000 | 15.0000 | 42.4674 | 15.8539 | 23.5636 | -49.3019 | 14.0702 | 18.5597 | 22.6206 |
| 0.2000 | 200.0000 | 21.0911 | 66.5250 | 15.1661 | 23.0012 | -70.1412 | 14.1421 | 20.0000 | 15.0000 | 42.4892 | 15.1661 | 23.0012 | -49.1248 | 13.6968 | 18.7602 | 21.0911 |
| 0.2125 | 212.5000 | 19.7625 | 64.3691 | 14.5615 | 22.5290 | -68.1894 | 13.7199 | 20.0000 | 15.0000 | 42.5001 | 14.5615 | 22.5290 | -48.9916 | 13.3541 | 18.9477 | 19.7625 |
| 0.2250 | 225.0000 | 18.5986 | 62.0265 | 14.0250 | 22.1287 | -66.0827 | 13.3333 | 20.0000 | 15.0000 | 42.5001 | 14.0250 | 22.1287 | -48.8913 | 13.0387 | 19.1258 | 18.5986 |
| 0.2375 | 237.5000 | 17.5733 | 59.4247 | 13.5458 | 21.7894 | -63.7569 | 12.9777 | 20.0000 | 15.0000 | 42.4784 | 13.5458 | 21.7894 | -48.8059 | 12.7480 | 19.2982 | 17.5733 |
| 0.2500 | 250.0000 | 16.6672 | 56.4322 | 13.1164 | 21.5051 | -61.0955 | 12.6491 | 20.0000 | 15.0000 | 42.4561 | 13.1164 | 21.5051 | -48.7479 | 12.4805 | 19.4705 | 16.6672 |
| 0.2625 | 262.5000 | 15.8683 | 52.7509 | 12.7324 | 21.2774 | -57.8351 | 12.3443 | 20.0000 | 15.0000 | 42.4235 | 12.7324 | 21.2774 | -48.7030 | 12.2360 | 19.6506 | 15.8683 |
| 0.2750 | 275.0000 | 15.1830 | 47.2415 | 12.3981 | 21.1354 | -52.9670 | 12.0605 | 20.0000 | 15.0000 | 42.3904 | 12.3981 | 21.1354 | -48.6737 | 12.0196 | 19.8646 | 15.1830 |
| 0.2875 | 287.5000 | 15.0000 | NaN | NaN | NaN | NaN | NaN | NaN | 15.0000 | NaN | NaN | NaN | NaN | NaN | NaN | 15.0000 |

(U) Figure 10 – Output data for aluminum (2.71 g/cc)

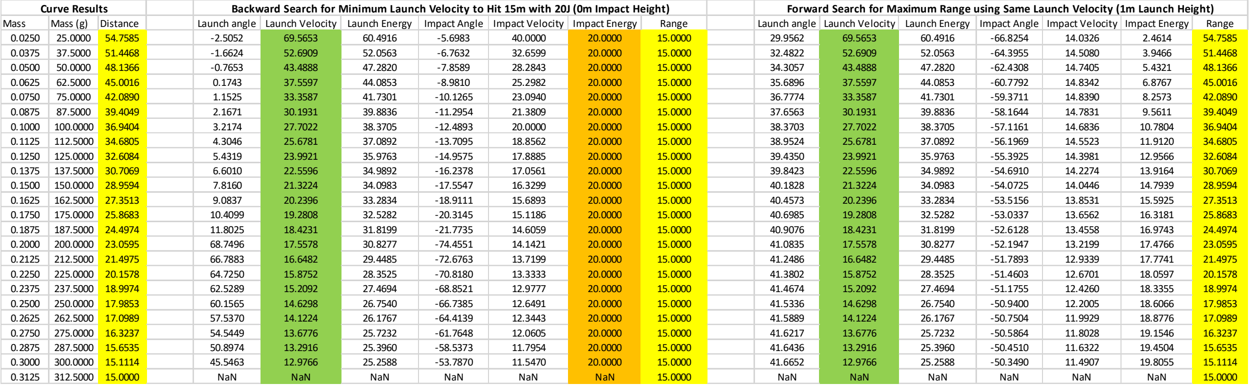

| Curve Results | | | Backward Search for Minimum Launch Velocity to Hit 15m with 20J (0m Impact Height) | | | | | | | Forward Search for Maximum Range using Same Launch Velocity (1m Launch Height) | | | | | | |
|---|---|---|---|---|---|---|---|---|---|---|---|---|---|---|---|---|
| Mass | Mass (g) | Distance | Launch angle | Launch Velocity | Launch Energy | Impact Angle | Impact Velocity | Impact Energy | Range | Launch angle | Launch Velocity | Launch Energy | Impact Angle | Impact Velocity | Impact Energy | Range |
| 0.0250 | 25.0000 | 54.7585 | -2.5052 | 69.5653 | 60.4916 | -5.6983 | 40.0000 | 20.0000 | 15.0000 | 29.9562 | 69.5653 | 60.4916 | -66.8254 | 14.0326 | 2.4614 | 54.7585 |
| 0.0375 | 37.5000 | 51.4468 | -1.6624 | 52.6909 | 52.0563 | -6.7632 | 32.6599 | 20.0000 | 15.0000 | 32.4822 | 52.6909 | 52.0563 | -64.3955 | 14.5080 | 3.9466 | 51.4468 |
| 0.0500 | 50.0000 | 48.1366 | -0.7653 | 43.4888 | 47.2820 | -7.8589 | 28.2843 | 20.0000 | 15.0000 | 34.3057 | 43.4888 | 47.2820 | -62.4308 | 14.7405 | 5.4321 | 48.1366 |
| 0.0625 | 62.5000 | 45.0016 | 0.1743 | 37.5597 | 44.0853 | -8.9810 | 25.2982 | 20.0000 | 15.0000 | 35.6896 | 37.5597 | 44.0853 | -60.7792 | 14.8342 | 6.8767 | 45.0016 |
| 0.0750 | 75.0000 | 42.0890 | 1.1525 | 33.3587 | 41.7301 | -10.1265 | 23.0940 | 20.0000 | 15.0000 | 36.7774 | 33.3587 | 41.7301 | -59.3711 | 14.8390 | 8.2573 | 42.0890 |
| 0.0875 | 87.5000 | 39.4049 | 2.1671 | 30.1931 | 39.8836 | -11.2954 | 21.3809 | 20.0000 | 15.0000 | 37.6563 | 30.1931 | 39.8836 | -58.1644 | 14.7831 | 9.5611 | 39.4049 |
| 0.1000 | 100.0000 | 36.9404 | 3.2174 | 27.7022 | 38.3705 | -12.4893 | 20.0000 | 20.0000 | 15.0000 | 38.3703 | 27.7022 | 38.3705 | -57.1161 | 14.6836 | 10.7804 | 36.9404 |
| 0.1125 | 112.5000 | 34.6805 | 4.3046 | 25.6781 | 37.0892 | -13.7095 | 18.8562 | 20.0000 | 15.0000 | 38.9524 | 25.6781 | 37.0892 | -56.1969 | 14.5523 | 11.9120 | 34.6805 |
| 0.1250 | 125.0000 | 32.6084 | 5.4319 | 23.9921 | 35.9763 | -14.9575 | 17.8885 | 20.0000 | 15.0000 | 39.4350 | 23.9921 | 35.9763 | -55.3925 | 14.3981 | 12.9566 | 32.6084 |
| 0.1375 | 137.5000 | 30.7069 | 6.6010 | 22.5596 | 34.9892 | -16.2378 | 17.0561 | 20.0000 | 15.0000 | 39.8423 | 22.5596 | 34.9892 | -54.6910 | 14.2274 | 13.9164 | 30.7069 |
| 0.1500 | 150.0000 | 28.9594 | 7.8160 | 21.3224 | 34.0983 | -17.5547 | 16.3299 | 20.0000 | 15.0000 | 40.1828 | 21.3224 | 34.0983 | -54.0725 | 14.0446 | 14.7939 | 28.9594 |
| 0.1625 | 162.5000 | 27.3513 | 9.0837 | 20.2396 | 33.2834 | -18.9111 | 15.6893 | 20.0000 | 15.0000 | 40.4573 | 20.2396 | 33.2834 | -53.5156 | 13.8531 | 15.5925 | 27.3513 |
| 0.1750 | 175.0000 | 25.8683 | 10.4099 | 19.2808 | 32.5282 | -20.3145 | 15.1186 | 20.0000 | 15.0000 | 40.6985 | 19.2808 | 32.5282 | -53.0337 | 13.6562 | 16.3181 | 25.8683 |
| 0.1875 | 187.5000 | 24.4974 | 11.8025 | 18.4231 | 31.8199 | -21.7735 | 14.6059 | 20.0000 | 15.0000 | 40.9076 | 18.4231 | 31.8199 | -52.6128 | 13.4558 | 16.9743 | 24.4974 |
| 0.2000 | 200.0000 | 23.0595 | 68.7496 | 17.5578 | 30.8277 | -74.4551 | 14.1421 | 20.0000 | 15.0000 | 41.0835 | 17.5578 | 30.8277 | -52.1947 | 13.2199 | 17.4766 | 23.0595 |
| 0.2125 | 212.5000 | 21.4975 | 66.7883 | 16.6482 | 29.4485 | -72.6763 | 13.7199 | 20.0000 | 15.0000 | 41.2486 | 16.6482 | 29.4485 | -51.7893 | 12.9339 | 17.7741 | 21.4975 |
| 0.2250 | 225.0000 | 20.1578 | 64.7250 | 15.8752 | 28.3525 | -70.8180 | 13.3333 | 20.0000 | 15.0000 | 41.3802 | 15.8752 | 28.3525 | -51.4603 | 12.6701 | 18.0597 | 20.1578 |
| 0.2375 | 237.5000 | 18.9974 | 62.5289 | 15.2092 | 27.4694 | -68.8521 | 12.9777 | 20.0000 | 15.0000 | 41.4674 | 15.2092 | 27.4694 | -51.1755 | 12.4260 | 18.3355 | 18.9974 |
| 0.2500 | 250.0000 | 17.9853 | 60.1565 | 14.6298 | 26.7540 | -66.7385 | 12.6491 | 20.0000 | 15.0000 | 41.5336 | 14.6298 | 26.7540 | -50.9400 | 12.2005 | 18.6066 | 17.9853 |
| 0.2625 | 262.5000 | 17.0989 | 57.5370 | 14.1224 | 26.1767 | -64.4139 | 12.3443 | 20.0000 | 15.0000 | 41.5889 | 14.1224 | 26.1767 | -50.7504 | 11.9929 | 18.8776 | 17.0989 |
| 0.2750 | 275.0000 | 16.3237 | 54.5449 | 13.6776 | 25.7232 | -61.7648 | 12.0605 | 20.0000 | 15.0000 | 41.6217 | 13.6776 | 25.7232 | -50.5864 | 11.8028 | 19.1546 | 16.3237 |
| 0.2875 | 287.5000 | 15.6535 | 50.8974 | 13.2916 | 25.3960 | -58.5373 | 11.7954 | 20.0000 | 15.0000 | 41.6436 | 13.2916 | 25.3960 | -50.4510 | 11.6322 | 19.4504 | 15.6535 |
| 0.3000 | 300.0000 | 15.1114 | 45.5463 | 12.9766 | 25.2588 | -53.7870 | 11.5470 | 20.0000 | 15.0000 | 41.6652 | 12.9766 | 25.2588 | -50.3490 | 11.4907 | 19.8055 | 15.1114 |
| 0.3125 | 312.5000 | 15.0000 | NaN | NaN | NaN | NaN | NaN | NaN | 15.0000 | NaN | NaN | NaN | NaN | NaN | NaN | 15.0000 |

(U) Figure 11 – Output data for high density polyethylene (0.95 g/cc)

## (U) Summary and Conclusions; Future Work

(U) The legacy and newly updated AOP-39 fragment projection curves which determine hazardous fragments for IM vulnerability assessments were discussed. The legacy curve was a 20J launch curve, representing the maximum distance a fragment could travel when launched with 20J, and therefore guaranteeing a launch energy in excess of 20J when the criterion is violated. Replacing this with a 20J impact curve would appear to make sense, however such curves become unbounded for smaller masses, which make their use undesirable. The characteristics of mass-distance curves are discussed, and it is shown that such curves lose accuracy and usefulness as the lethality criterion becomes less conservative. Thus the new curve is a 20J impact at 15m criterion which was shown to manage these difficulties. This curve guarantees that a fragment which violates the criterion was launched in excess of the minimum velocity to impact 15m with 20J. This criterion results in slightly larger throw distances than the 20J launch curve, which is constructed similarly. In addition lethality criteria are discussed. 20J is thought by some to be qualitatively conservative enough for the mass-distance curve to be meaningful, while at the same time being hazardous enough to pose some risk of nonlethal blunt injury. However more lethality modeling should be performed for this set of masses and materials. The criterion is currently of significant consequence to the success or failure of various IM programs, and it is hoped that better understanding of this criterion and its characteristics can result in improved interpretation and development of IM tests and standards.

## (U) References

[1] "Department of Defense Ammunition and Explosives Hazard Classification Procedures". Joint Technical Bulletin TB-700-2, 1998.

[2] "Guidance on the Assessment and Development of Insensitive Munitions". NATO Allied Ordnance Publication AOP-39 (Edition 3), 2010.

[3] McCoy, R. L. *Modern Exterior Ballistics: The Launch and Flight Dynamics of Symmetric Projectiles*. Atglen, PA: Schiffer Publishing Ltd., 2008.

[4] Swisdak, M. M. "Fragmentation Effects: An Overview". In R. A. Scott (Ed.), *Design Considerations for Toxic Chemical and Explosives Facilities*. Washington, DC: ACS Symposium Series, American Chemical Society, 1987.

[5] Montanaro, P. E. "TRAJ – A Two Dimensional Trajectory Program for Personal Computers". Naval Surface Warfare Center, 1990.

[6] Zaker, T. A. "Fragment and Debris Hazards". DDESB TP-12, 1975.

[7] Shampine, L. F. "The MATLAB ODE Suite". SIAM Journal on Scientific Computing, 1997.

[8] Miers, K. T. "Insensitive Munitions Type IV Fragment Projection Energy Threshold". 63rd JANNAF Propulsion Hazards Subcommittee Meeting. Newport News, VA, 2016.

[9] Van Der Voort, M., Baker, E., Schultz, E., Sharp, M. "Projection Criteria for Insensitive Munitions and Hazard Classification". Insensitive Munitions & Energetic Materials Technology Symposium, Nashville, TX, 2016.

[10] Gill, P. E. *Practical Optimization*. San Diego, CA: Academic Press, Inc., 1981.

[11] Baker, E. L. Private Communication. NATO Munitions Safety Information Analysis Center, 2016.